

# Force measurements in positive unipolar wire-to-plane corona discharges in air

Victor de Haan

BonPhysics B.V., Laan van Heemstede 38, 3297 AJ Puttershoek, The Netherlands, e-mail: [victor@bonphysics.nl](mailto:victor@bonphysics.nl)

Received: date / Revised version: date

**Abstract.** Measurements of force generated by a positive unipolar wire-to-plane corona discharge in air are compared with numerical simulations. The generated force does not depend on the ion or electron mobilities, preventing the influence of uncertainty and variation of these parameters. A method is described to simulate the voltage and charge distribution for a wire-to-plane set-up. This method enables the determination of the transition between unipolar and bipolar discharges. In the experimental set-up breakdown electric field of air reduces with increasing discharge current.

**PACS.** 02.60.Cb Numerical simulation; solution of equations – 02.70.Bf Finite-difference method – 52.80.Hc Glow; corona

## 1 Introduction

Atmospheric pressure corona discharges in air are important for use as electrostatic precipitators, ozone generators [1], thunderclouds [2], mass transport [3] and so on. An upcoming field is the use of corona discharge to generate electric winds for cooling purposes [4]. The physics of corona discharge however is not fully understood. Peek [5] was one of the first to study the phenomenon in a systematic way. He found the onset breakdown electric field at the wire surface of a wire-cylinder discharge corresponds to

$$E_a = f E_o \delta \left( 1 + \sqrt{\frac{a_o a}{a \delta}} \right), \quad (1)$$

where  $f$  is an irregularity factor (for polished copper wire  $f \approx 1$ ),  $E_o$  the breakdown electric field of air equal to 31 kV/cm,  $\delta$  the relative density of the air compared to the density of air at 25 °C and 1013 kPa,  $a$  the wire radius and  $a_o$  a constant equal to 0.0949 cm. In this paper the outer edge of the corona is defined as the distance to the center of the wire,  $r_c$  where the electric field equals the breakdown electric field. In the corona between wire surface and outer corona edge it is assumed that space charge has negligible influence on the electric field. This is a valid assumption as close to the wire the electric field gradient is already very large due to geometry. Then, according to equation (1) the corona size is given by

$$r_c = a + \sqrt{\frac{a_o a}{\delta}}. \quad (2)$$

This can be calculated by using equation (11) with  $\alpha(x) = 1$ . The second term at the right hand side of this equation represents the ionisation sheath. In this sheath the

discharge is carried by electrons, positive and negative ions [6]. Outside this sheath the discharge is mainly unipolar. A recent overview of possible electrical breakdown criteria has been given by Lowke [7]. He couples  $a_o$  to the discharge parameters of air

$$a_o = \frac{\ln(Q)}{(E_o/N_o)^2 N_o B}, \quad (3)$$

where  $Q$  is the number of ionisations to occur to sustain breakdown,  $N_o$  is the air number density at 25 °C and 1013 kPa and  $B$  is  $1.35 \times 10^{16} \text{ V}^{-2} \text{ m}^{-2}$ <sup>1</sup>.  $Q$  depends on the corona discharge mechanism. He suggests a possible mechanism for the onset corona discharge but does not take into account the effect of space charge in the air surrounding the corona. Normally this is not a problem as measurements of the breakdown electric field of air are mostly done for relatively small space charges at relatively small discharge currents. However, for the above-mentioned applications the breakdown electric field in the presence of a discharge current is important. Additional problems are the relative uncertainties of the mobility of the involved ions and electrons. In the following it is shown that the force generated by a wire-to-plane corona discharge is independent of charge carrier mobilities. This force only depends on the applied potential difference between wire and plane and the geometry of the discharge. Force measurements were performed to determine the influence of space charge on the breakdown electric field of air at atmospheric pressure and to eliminate the influence of the charge carrier mobilities. In the following this

<sup>1</sup> Lowke uses  $B=2.08 \times 10^{16} \text{ V}^{-2} \text{ m}^{-2}$ , but he takes 25 kV/cm for the breakdown electric field of air.

method is described and measurements for several geometries are presented and discussed.

## 2 Outline of the method

The method is based on solving the Poisson equation for certain geometry combined with the continuity equations for ion and electron flow. Solving Poisson equation gives the potential distribution,  $U$  and the continuity equations give the space charge distribution,  $\rho$ . In air (the relative permittivity,  $\epsilon_r$  is approximated by 1) the Poisson equation is

$$\nabla^2 U = -\frac{\rho}{\epsilon_0} \quad (4)$$

where  $\epsilon_0$  is the permittivity of free space. For each charge species  $i$ , being positive or negative ions or electrons, the stationary continuity equation is

$$\nabla \cdot \mathbf{J}_i = 0 \quad (5)$$

where  $\mathbf{J}_i$  is the current density of charge species  $i$ . It is assumed that no transformation from one species into another occurs. If the mobility,  $\mu_i$  of the species does not depend on either space charge nor electric field,  $\mathbf{E} = -\nabla U$  it is given by

$$\mathbf{J}_i = \mu_i |\rho_i| \mathbf{E} \quad (6)$$

where  $\rho_i$  is the charge density of species  $i$ . Hence, equation (5) reduces to

$$\rho_i \nabla \cdot \mathbf{E} + \mathbf{E} \cdot \nabla \rho_i = 0 \quad (7)$$

Adding all equations (7) results in the continuity equation for the total space charge

$$\rho \nabla \cdot \mathbf{E} + \mathbf{E} \cdot \nabla \rho = 0 \quad (8)$$

The force exerted by the electric field on a point particle with charge  $q$  is by definition  $\mathbf{F} = q\mathbf{E}$ . This can be extended to find the force exerted by the electric field on a charge density distribution in a volume  $V$ :

$$\mathbf{F} = \int \rho \mathbf{E} dV \quad (9)$$

Neither equation (4) nor (8) contains any reference to the mobility of the involved ions or electrons, other than that they are constant. The simultaneous solution of these equations results in voltage and charge density distributions independent of these parameters. Hence according to equation (9) the force exerted by the charge distribution does not depend on the mobilities. Further, this force is uniquely determined by the applied voltage difference between wire and plane and the geometry. The electric current,  $\mathbf{I}$  through some flat area  $A$  is given by

$$\mathbf{I} = \sum_i \int \mathbf{J}_i \cdot \mathbf{n} dA = \sum_i \int \mu_i |\rho_i| \mathbf{E} \cdot \mathbf{n} dA \quad (10)$$

where  $\mathbf{n}$  is the normal to area  $A$ . The current consists of contributions from all charge species. Hence, it is much more difficult to calculate accurately than the force. Further, if the total charge distribution consists of positive and negative species, the current increases as indicated by the absolute sign.

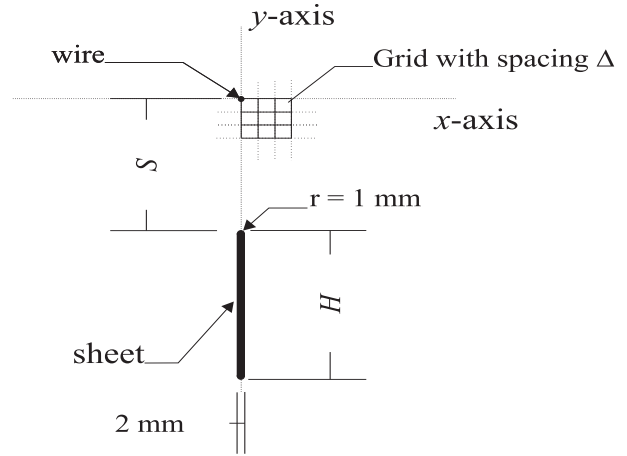


Fig. 1. Sketch of a cross section of the wire-to-plane geometry

## 3 Experimental set-up

The detection of force exerted by a space charge distribution needs equation (9) to produce a result different from 0. This can be achieved by an asymmetrical corona discharge, like a wire-to-plane discharge. Normal the wire is put above and parallel to the plane. Then, the electric wind generated by the space charge will push against the plane and reduce the measurable force [8]. To overcome this problem, the plane is reduced to a sheet and the wire is put parallel to the sheet at a distance  $S$ . The wire is positioned in the same plane as the sheet.  $H$  is the height of the sheet (4.0 cm in the experiments). This configuration is shown in figure 1. Sheet thickness was 2 mm, far less than either  $S$  or  $H$ . The upper and lower end of the sheet were smoothly rounded with a radius of 1 mm to as much as possible avoid production of opposite signed charges. The length of both wire and sheet was 53.5 cm. In the experiment  $S$  was varied between 2.0 and 6.0 cm with steps of 1.0 cm. Wires of different radius  $a$  were used: 0.040, 0.0635, 0.075, 0.10, 0.1575 and 0.25 mm. Measurements were performed at atmospheric conditions:  $20 \pm 1$  °C and  $1013 \pm 10$  kPa. Relative humidity was between 0.5 and 0.8. The force was measured by the reduction of weight of the set-up with a lever. One arm of the lever was connected with light non-conducting wires attached to the set-up. The length of these wires was about 50 cm ensuring the influence of the surroundings was negligible. The other arm was rigidly connected to a balance with a range of 100 gram and an accuracy of 0.1 gram. The ratio of the length of the arms of the lever was 1:10. This lever enabled force measurements between 0 and 100 mN with an accuracy of 0.1 mN. The measurements were done with increasing and decreasing voltages to check for systematic deviations. A DC high voltage between 0 and 30 kV was applied to the wire while the sheet was grounded. An amperere meter monitored the current supplied by the high voltage power supply.

## 4 Simulation

To simulate the electric field a model was developed following [9]. First, the problem is reduced to 2 dimensions by assuming an infinitely long wire and sheet. Second, the problem is made periodic in both  $x$ - and  $y$ -directions with a period of  $2W_x$  and  $W_y$  respectively.  $2W_x$  respectively  $W_y$  being the distance in  $x$ -respectively  $y$ -direction between two adjacent set-ups.  $x = W_x$  and the  $x = 0$  are symmetry axis. If  $W_x$  and  $W_y$  are large enough the results can be applied to a single set-up. Here,  $W_x$  and  $W_y$  are chosen optimizing the computation time and required accuracy. Third, the problem is discretized by assuming a square grid with spacing  $\Delta$ . The number of grid lines in the  $x$ -direction,  $n$  equals  $W_x/\Delta + 1$ , the number in the  $y$ -direction,  $m$  equals  $W_y/\Delta$ . Fourth, the appropriate boundary conditions are defined and the discretized version of equations (4) and (8) are solved sequentially until a stable solution is found. For the solution of the discretized Poisson equation a Poisson solver was used based on the linear conjugate gradients method [10]. For the solution of the discretized continuity equation a non-linear conjugate gradient method was used [11]. The appropriate boundary conditions are not evident. At the sheet the potential was simply set to 0. At the wire position however, the wire radius had to be taken into account. As the wire radius is very small compared with the grid size a method had to be devised to take it into account. The method as described in [9] was used and extended to incorporate unipolar space charge around the wire. Around the wire up to the first adjacent grid point cylindrical geometry is assumed. This is justified as  $\Delta \ll S$ . The space charge density at  $r = r_c$  is taken to be  $\rho_c$ . Then, the electric field and charge density near the wire are given by

$$E(r) = fE_o\delta\frac{\alpha(r/r_c)}{r/r_c}, \quad (11)$$

$$\rho(r) = \frac{\rho_c}{\alpha(r/r_c)}, \quad (12)$$

where  $\alpha(x) = \sqrt{1 + \eta(x^2 - 1)}$  if  $x \geq 1$  and  $\alpha(x) = 1$  if  $x < 1$  and  $\eta = \rho_c r_c / fE_o\delta\epsilon_o$  is a measure for the total space charge at the outside of the corona ( $r = r_c$ ). For a unipolar discharge (outside of the corona)  $\eta$  is proportional to the discharge current,  $I$

$$\eta = \frac{I/L}{2\pi\mu\epsilon_o(fE_o\delta)^2}, \quad (13)$$

where  $\mu$  is the mobility of the unipolar charge carriers. Note that  $\eta$  is determined by the experimental conditions only. A graph of the electric field as function of  $r$  for several  $\eta$  is shown in figure 2. The theoretical maximum value for  $\eta$  is 1. For  $\eta = 1$  the electric field in the whole gap equals the breakdown electric field and there is no way to prevent spark discharge. For  $r/r_c < 1$  the lines coincide. Inside the corona the electric field gradient due to the space charge density is negligible compared to the geometric gradient. For all experiments  $\eta < 0.05$ , so the influence of the space charge on the electric field is negligible near the wire up

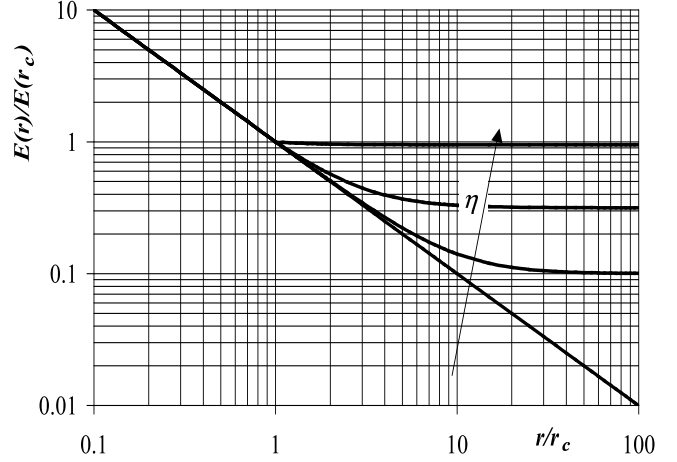


**Fig. 2.** Ratio of electric field,  $E(r)$  to electric field at corona edge,  $E(r_c)$  as function of distance to center of wire,  $r$  for  $\eta = 0; 0.01; 0.1$  and  $0.9$ . The arrow indicates increasing values of  $\eta$ .

to  $r = 5r_c$ . Hence, the exact shape of the streamers in the corona area is not important for the results presented here. The voltage drop from wire to outer edge of the corona is given by

$$\Delta U_c = -fE_o\delta r_c \ln \frac{r_c}{a}, \quad (14)$$

independent of  $\eta$ . The voltage drop from outer corona edge to a radius of  $r > r_c$  is given by

$$\Delta U(r) = -fE_o\delta r_c \left( \alpha\left(\frac{r}{r_c}\right) - 1 + \chi\left(\frac{r}{r_c}\right)\sqrt{1-\eta} \right), \quad (15)$$

where

$$\chi(x) = \ln \left\{ \frac{\sqrt{1-\eta} + 1}{\sqrt{1-\eta} + \alpha(x)} x \right\}. \quad (16)$$

This function is shown in figure 3 for different values of  $\eta$ . Note the positive values for the voltage drop as  $r/r_c < 1$ . Here,  $\Delta U(r) = -fE_o\delta r_c \ln(r/r_c)$ , again independent of  $\eta$ . For the boundary conditions at the wire the electric field at all grid positions adjacent to the wire is made equal to  $E(\Delta)$  and the space charge density is set to  $\rho(\Delta)$ .

## 5 Results and discussion

The wire voltage was calculated by adding  $\Delta U(\Delta) + \Delta U_c$  to the average of the voltage at the wire adjacent grid points. From the simulations the spread in the voltages at these grid point was only a few percent. This indicates the accuracy of the assumption of cylindrical geometry near the wire up to the first grid point.  $f$  was determined by fitting the onset breakdown electric field to equation (1). For the onset  $r_c$  was calculated with equation (2). As an example, the onset voltage distribution for  $S = 3.0$  cm and  $a = 0.040$  mm is shown in figure 4. The position of

$S$ cm	$W_y$ cm	$W_x$ cm	$\Delta$ mm	$a / \text{mm}$ 0.040	0.0635	0.075	0.10	0.1575	0.25
2.0	20.0	10.0	2.0	0.88	0.89	0.87	0.87	0.86	0.85
3.0	33.0	12.0	3.0	0.90	0.90	0.83	0.83	0.90	0.85
4.0	40.0	20.0	4.0	0.85	0.78	0.88	0.88	0.91	0.85
5.0	50.0	25.0	5.0	0.80	0.80	0.85	0.85	0.81	0.95
6.0	60.0	30.0	6.0	0.80	0.80	0.80	0.80	0.90	0.95
average				0.86(4)	0.84(5)	0.84(5)	0.86(2)	0.86(2)	0.88(2)

**Table 1.** Fitted irregularity factor  $f$  and simulation parameters for all geometries.  $f$  was fitted to match the measured onset electric field at the wire position with equation 1.

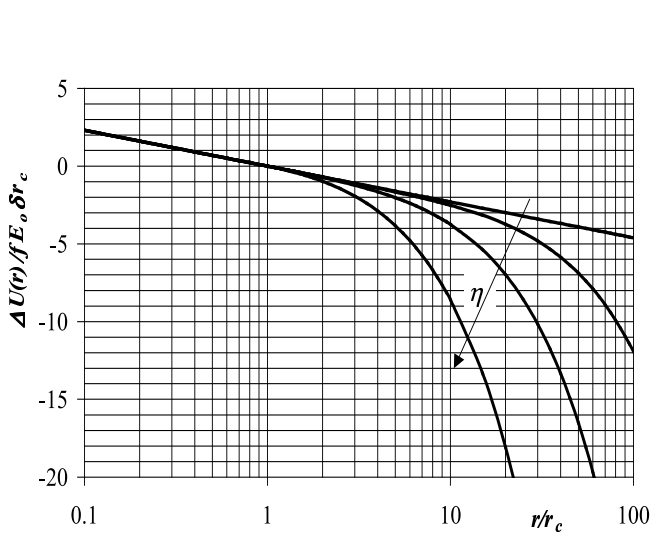


**Fig. 3.** Normalized voltage drop  $\Delta U(r)/fE_0\delta r_c$  as function of distance to wire center,  $r$  for  $\eta = 0; 0.01; 0.1$  and  $0.9$ . The arrow indicates increasing values of  $\eta$ .

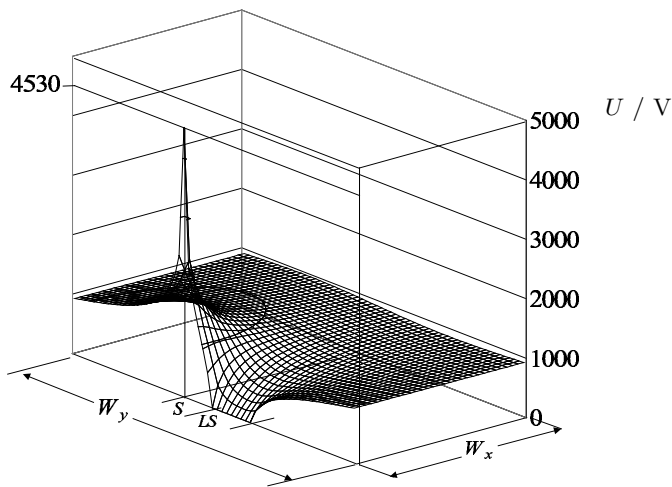


**Fig. 4.** Voltage distribution,  $U$  at the onset voltage for  $S = 3.0$  cm,  $LS = 4.0$  cm and  $a = 0.040$  mm. Grid size was  $5.0$  mm;  $W_x = 15.0$  cm;  $W_y = 30.0$  cm. Wire onset voltage =  $5.82$  kV.

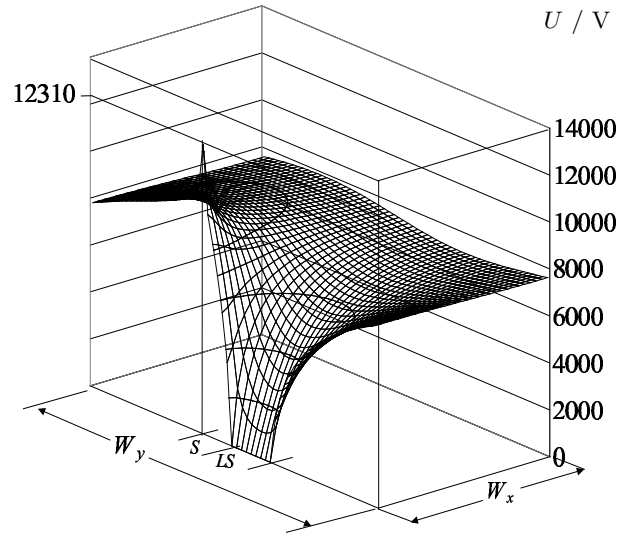


**Fig. 5.** Voltage distribution,  $U$  for  $\rho_c = 128 \mu\text{Cm}^{-3}$  and same dimensions as in figure 4. Wire voltage =  $13.6$  kV.

the wire and sheet are evident. Notice the steep rise at the wire position. The wire onset voltage was  $5.82$  kV. In this case the corona radius according to equation (2) is  $0.235$  mm. The corona voltage drop according to equation (14) was ( $f = 1$ )  $1290$  V. In the simulation the voltage at the wire position equals the voltage at the outside of the corona. Hence, in the simulation the voltage at the wire position was  $4.53$  kV. The fitted irregularity factors are shown in table 1. The onset voltages varied between  $5$  and  $12$  kV. The average irregularity factor is  $0.86$ , this indicates that the used value of  $E_0$  is slightly too high. Using a value of  $27$  kV/cm instead of  $31$  kV/cm, increases the average irregularity factor to  $0.99$ . The small spread in the fitted value of the irregularity factor is evidence for the correctness of the performed simulation. Using these irregularity factors, at every measured voltage and geometry the simulated force was fitted to the measured one by adjusting  $r_c$  and  $\rho_c$ . Both parameters are needed to determine the force at a certain voltage and geometry. All other parameters were taken from the experimental conditions. Figure 5 shows an example of a voltage distribution for  $\rho_c = 128 \mu\text{Cm}^{-3}$  (which corresponds to a unipolar discharge current of  $0.1$  mA/m, if  $\mu = 2.0 \text{ cm}^2\text{V}^{-1}\text{s}^{-1}$ ) with the same geometry as in figure 4. Figure 6 shows an example of the corresponding space charge density distri-

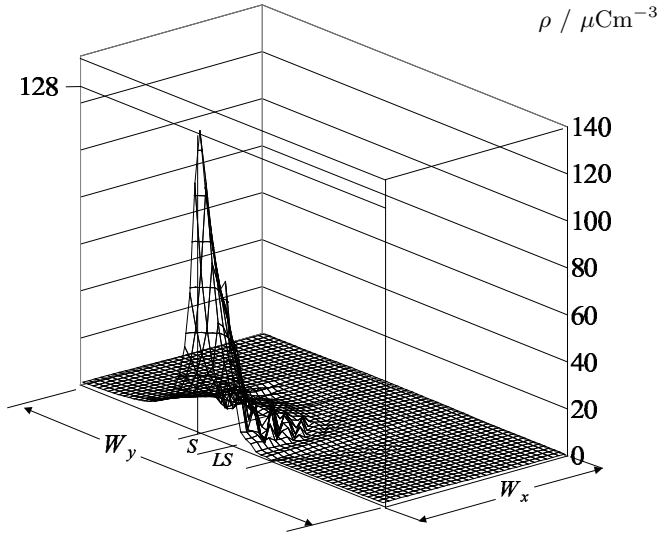


**Fig. 6.** Charge density distribution,  $\rho$  for  $\rho_c = 128 \mu\text{Cm}^{-3}$  and same dimensions as in figure 4. Wire voltage is 13.6 kV.

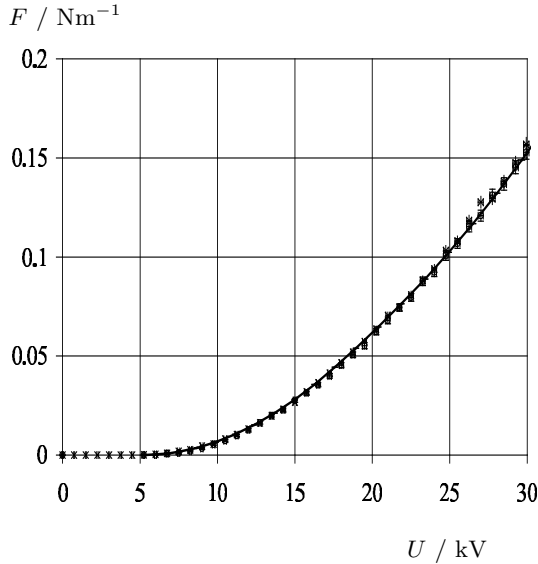


**Fig. 7.** Exerted force,  $F$  as function of wire voltage,  $U$  for same dimensions as figure 4. The symbols with error bars represent the measurements for increasing (crosses) and decreasing (circles) voltage. The lines represent the simulated results.

bution. Notice the small oscillations in the current density. This is due to the limited accuracy of the calculations and the accuracy of discretization. It is assumed they do not significantly change the results presented here. Simulations and measurements of the exerted force for the above-mentioned geometry as a function of applied wire voltage are shown in figure 7. The symbols with error bars represent the measurements for increasing and decreasing voltage. The lines represent the simulated results. The fitted force matches the measurement accurately. The discharge current is calculated using the voltage and charge distributions and equation (10) applied for a unipolar current with a mobility of  $2.0 \text{ cm}^2\text{V}^{-1}\text{s}^{-1}$ . This is shown in

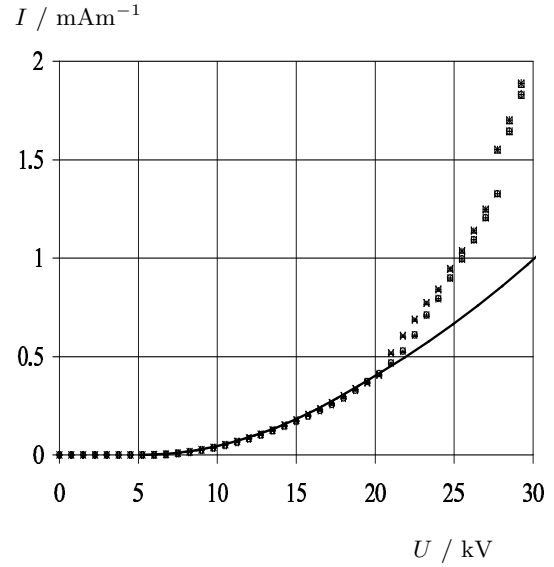


**Fig. 8.** Discharge current,  $I$  as function of wire voltage,  $U$  for same dimensions as figure 4. The symbols with error bars represent the measurements for increasing (crosses) and decreasing (circles) voltage. The lines represent the simulated results.

figure 8. For small voltages the deviation with the measurements are within the accuracy of the measurements. Note that both force and discharge current measurements are accurately calculated with the same space charge density distribution. For the force this is a result of the fit. For the discharge current this is not evident, as the currents were not used in the fits. Force is a volume and current an area integral over a charge and electric field distribution corresponding to equation 9 and 10 respectively. Hence, good agreement between the measured and simulated discharge current is a further indication of the validity of this method. For larger voltage the measured discharge current grows faster than the simulated one. Here, the current measurements with increasing and decreasing voltage starts to deviate slightly. This is caused by a change of the discharge from unipolar to bipolar. The charges of the other sign reduce the force but enhance the current. From the fitted  $r_c$  the corresponding values of  $\sqrt{a_o}$  are calculated using equation (2). They are shown in figures 9 and 10. The vertical lines in the graphs show the maximum force for which the simulated current matched the measured one. This is the maximum force for a unipolar discharge in the specified geometry.  $\sqrt{a_o}$  decreases from the onset value of  $0.0308 \text{ m}^{0.5}$  more or less linear with a slope dependent on the geometry. The slope is proportional to  $S$ . For different wire diameters the slope is approximately the same. The reduction of  $\sqrt{a_o}$  corresponds to a reduction of the electric field at the wire position. In literature this is attributed to a reduction of the breakdown electric field of air dependent on the applied over voltage [12,13]. The physics behind this are not yet understood. The reduction of  $\sqrt{a_o}$  to 0 corresponds, according to equation (3), to a reduction of  $Q$  to 1. The number of needed ionisations reduces to 1. The slope's indepen-

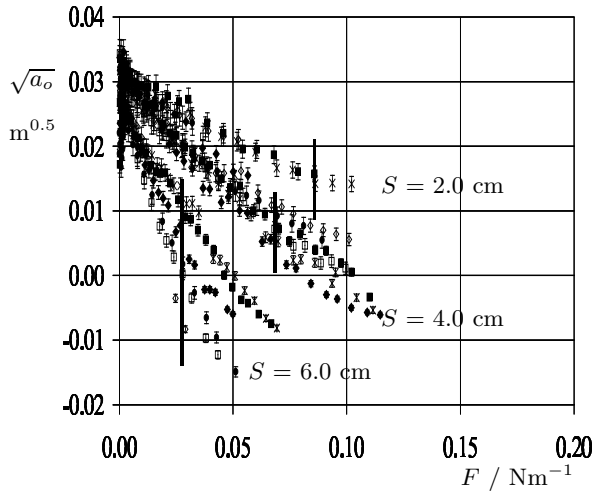


**Fig. 9.** Calculated  $\sqrt{a_o}$  as function of measured force  $F$  for measured geometries with  $S = 2.0$ ; 4.0 and 6.0 cm. Closed diamonds:  $a=0.040$  mm; closed squares:  $a=0.0635$  mm; stars:  $a=0.075$  mm; open diamonds:  $a=0.10$  mm; open squares:  $a=0.1575$  mm and dots:  $a=0.25$  mm. Error bars are estimates of accuracy of simulation. The vertical lines indicate the maximum force for which the discharge is unipolar.

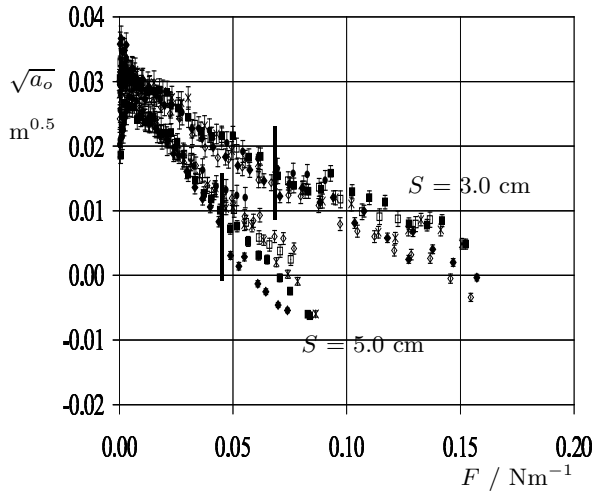


**Fig. 10.** Calculated  $\sqrt{a_o}$  as function of measured force  $F$  for measured geometries with  $S = 3.0$  and 5.0 cm. See figure 9 for details.

dence of  $a$  and its proportionality to  $S$  suggest  $Q$  depends on the total amount of charge present in the discharge and not on local conditions around the wire. Lowke proposes the breakdown of air is caused by ions produced by interaction of metastable molecules. The effect presented here supports his conclusion, as the number of metastable molecules present in the air depends on the charge density. The measurements presented here are not accurate enough to determine the mechanism of this dependence. For larger forces, where the discharge becomes bipolar,  $\sqrt{a_o}$  becomes negative, indicating the limit of equation (8). This equa-

tion assumes no transformation of one charge species into another. This is further supported by the observed trend that for larger interaction times of the charge species (i.e. for large traveling distance of the charges)  $\sqrt{a_o}$  becomes negative for smaller forces.

## 6 Conclusions

Force generated by an asymmetrical wire-to-plane discharge can be measured and accurately simulated. Comparison of measurements of both force-voltage and current-voltage characteristics with finite differences simulations show good agreement for the unipolar region. These measurements can be used to determine the transition voltage of an unipolar into a bipolar discharge. Further, it is possible to determine the breakdown electric field of air dependent on the discharge conditions. The presented measurements are in qualitative agreement with the breakdown mechanism as proposed by Lowke, but measurements are not accurate enough to determine the dependence of this mechanism on the space charge density distribution.

The author wishes to thank Mrs. G. Gravendeel-van Ingen for a valuable contribution to the experimental set-up.

## References

1. Chen J and Davidson J H, Plasma chemistry and plasma processing **22** No 4, (2002) 495-522
2. Aleksandrov N L, Bazelyan E M, Carpenter Jr R B, Drabkin M M and Raizer Y P, J. Phys. D: Appl. Phys. **34**, (2001) 3256-3266
3. Sigmond R S and Lagstad I H, High Temp. Chem. Processes **2**, (1993) 221-229
4. Schlitz D J and Garimella S V, ASME National Heat Transfer Conference, July 2004, (2004) (in review)
5. Peek F W, Dielectric Phenomena in high voltage engineering (Mc Graw-Hill Book Company Inc., New York 1915 )
6. Chen J and Davidson J H, Plasma chemistry and plasma processing **22** No 4, (2002) 199-224
7. Lowke J J and Alessandro F D, J. Phys. D: Appl. Phys. **36**, (2003) 2673-2682
8. Béquin Ph, Castor K and Scholten J, Eur. Phys. J. AP **22**, (2003) 41-49
9. McDonald J R, Smith W B, Spencer III H W and Sparks L E, Journal of Applied Physics **48** No 6, (1977) 2231-2243
10. Shewchuk J R, An introduction to the conjugate gradient method without the agonizing pain (Pittsburgh: School of Computer Science, Carnegie Mellon University, Pittsburgh PA 15213 USA 1994 )
11. Bjoerk A, Acta Numerica, (2004) 1-51
12. Jaiswal v and Thomas M J, J. Phys. D: Appl. Phys. **36**, (2003) 3089-3094
13. Aboelsaad M M, Shafai L and Rashwan M M, IEE Proceedings **136** Pt. A No 1, (1989) 33-40